Title
Arp2/3 directly interacts with DNA through the p41 subunit and is involved in the non-homologous end joining repair pathway

Author
Lee, Terri

Publication Date
2020

Peer reviewed|Thesis/dissertation

Arp2/3 directly interacts with DNA through the p41 subunit and is involved in the non-homologous end joining repair pathway

by
Terri Lee

DISSERTATION
Submitted in partial satisfaction of the requirements for degree of
DOCTOR OF PHILOSOPHY

in

Biochemistry and Molecular Biology

in the

GRADUATE DIVISION
of the
UNIVERSITY OF CALIFORNIA, SAN FRANCISCO

Approved:

DocuSigned by:
Dyche Mullins
E4FB70A20A7546F...

Dyche Mullins
Chair

DocuSigned by:
Wallace Marshall
[illegible]

Wallace Marshall

DocuSigned by:
David Toczyski
B39DA64A208E4CB...

David Toczyski

Committee Members

Acknowledgements

I am grateful for my family for not questioning my decision to go to graduate school and for being supportive of my choices. But forever questioning if I'm eating well or sleeping enough, and maybe when I would graduate and get a job.

I'm incredibly grateful for Dyche as an advisor. His commitment to allow each student to find their own path has facilitated much of my best life decisions, both scientifically and career-wise. I am forever grateful for being allowed the experiences I had, so thank you.

I'd like to thank my official thesis committee members, Wallace Marshall and Dave Toczyski, for their support and advice during graduate school. I'd also like to thank the unofficial thesis committee members who were found in Genentech Hall hallways and in line at Café 24.

Graduate school is one of the toughest experiences and often times feels like an exercise in masochism. But it's not an experience or choice I regret. Going to lab every day and being in lab during those weeks where you spend more time in lab than not… I'm glad I had a fantastic group of labmates who made those times easier. Early afternoons (late mornings??) at the Anchor Steam Brewery were some of the best ways to spend/end a lab day. And finding random treasures strewn about lab from previous years' excursions has always been delightful. I'm proud of the unverified fact that we have the highest lava lamp population in the county.

Perhaps the first masochistic endeavor was signing up to work at the Marine Biological Laboratory in the summer of 2009, under the tutelage of Dyche and Clare (and Bob). It was there, during the feverish late nights on secret beaches and blurry transitions from night to morning on damp wooden piers that I committed to science/chaos (and ultimately to UCSF). Some of my greatest memories and friendships have come from those Woods Hole summers, and I'm grateful for those experiences and people.

I'd like to thank the folks at Gladstone and also at MPM Capital for letting me dabble in dealings I had no business doing and taking a chance on me. It was a more than productive distraction that kept me sane during the difficult times in graduate school.

I'm grateful for all my friends, even if some of us have grown apart, I appreciate the adventures we had together. They made graduate school a lot more bearable and I hope we all achieve what we seek to in this post-graduate world. I'm forever grateful for my post-graduate friends who would always be down to commiserate and tell me that things will pass, and to just do it. They didn't warn me nearly enough about the weird depression spiral that comes at the end, but that's okay, I'm still grateful and I forgive them.

Lastly, I'd like to thank Scott for being an amazing source of joy these last few months. I'm happy to have found you. You'll always be one of the good things that came out of this pandemic. I'm glad this is working out so well even though you've never watched a single Hellraiser movie before meeting me. I think I'm done secret crying downstairs and am ready for that 1000-piece puzzle now.

Arp2/3 directly interacts with DNA through the p41 subunit and is involved in the non-homologous end joining repair pathway

Terri Lee

ABSTRACT

Nuclear actin filaments and actin regulators play a role in the DNA repair process. The branched actin nucleator Arp2/3 has been identified as one such actin regulator and was found to localize to DNA double-stranded break sites and play a role in efficient homology-directed repair. Arp2/3's cytoplasmic activities have been well-documented and studied, but its presence in the nucleus is only beginning to be understood. We asked whether Arp2/3 was binding directly to DNA for its role in DNA repair and whether it also played a role in the non-homologous end joining DNA repair pathway. We find that Arp2/3 binds directly to DNA and that binding is facilitated by its p41 subunit, with a preference for the p41b isoform. Additionally, this binding is mutually exclusive of Arp2/3's ability to bind the VCA domain of its activator, leading to Arp2/3's actin nucleating abilities remaining intact. In addition to the previously reported role of Arp2/3 in homology-directed repair, we present evidence that Arp2/3 is also required for effective non-homologous end joining.

Table of Contents

List of Figures

List of Tables

1. INTRODUCTION

Actin is an important cytoskeletal protein, first discovered as part of the contractile apparatus of mammalian muscle (Straub, 1942). Twenty years after its discovery in muscle, actin was found in non-muscle cells (Hatano and Oosawa, 1966), where it is now known to support many fundamental biological processes, including: locomotion, division, phagocytosis, endocytosis, and membrane trafficking (Pollard et al, 2000; Pollard and Borisy, 2003; Lee and Dominguez, 2010). Nine years after it was identified outside of muscle, actin turned up in another unexpected place: inside the nucleus (LeStourgeon et al., 1975). Nuclear actin has since been spotted in many cell types and linked to many nuclear processes (Pederson and Aebi, 2002), but our understanding of what actin does inside the nucleus has lagged far behind our understanding of its cytoplasmic functions.

Recently developed tools now enable direct observation (Belin et al., 2013; Belin et al., 2014; Plessner et al., 2015; Du et al., 2015; Treisman, 2013) and perturbation (Stuven et al., 2003; Bohnsack et al., 2006; Dopie et al., 2012) of nuclear actin, without affecting the cytoplasmic actin cytoskeleton. Studies using these new tools are beginning to provide a clearer picture of the functions of nuclear actin and the molecules that control its transport and assembly. In a recent study published in the journal eLife (Belin et al., 2015), for example, we found that DNA damage induces assembly of nuclear actin filaments that accelerate DNA repair. Although the mechanism(s) by which actin influences DNA repair remain unclear, we do know that DNA damage induces actin filament formation via the activity of two well-known actin regulators, Formin-2 (FMN2) and Spire.

The evolution of multicellular complexity not only increased the number of processes an organism performs and the specificity of cellular/tissue roles, but also increased the target size for DNA damage. Damage to one or too many cells compromises the entire organism, thus, a need for more sophisticated DNA repair methods evolved with multicellularity. DNA double strand breaks (DSB) are the most detrimental type of DNA lesion that occur, and if left

unrepaired, jeopardize the genomic integrity and vitality of a cell. A successful DNA damage response requires the cell to sense the DSB, process it for repair, and then either repair or bypass it. Homologous recombination (HR) and Non-Homologous End Joining (NHEJ) are the two major DSB repair pathways in mammalian cells. HR involves resection of the DNA lesion and use of a homologous sequence as the repair template, while NHEJ repair does not require a template to directly re-ligate the break ends (Iliakis et al., 2019). DNA repair is important for an organism's survival, as DNA damage occurs on a regular basis, therefore the cell's ability to repair itself efficiently and with high fidelity is imperative. The increasing role of actin and its nucleators in the DNA repair process has become more and more evident, with the discovery of actin nucleators trafficking into the nucleus upon DNA damage to regulate transcription or potentially play a more direct role at the sites of DNA damage (Zuchero et al, 2012, Baarlink and Grosse, 2014; Hurst et al., 2019), in addition to actin regulators and nucleators present in the nucleus under normal conditions.

Roughly speaking, three types of molecules make new actin filaments from scratch in the cytoplasm: the Arp2/3 complex, formin-family proteins, and actin monomer-binding proteins such as spire. The Arp2/3 complex creates branched actin networks, whereas formins and spires create unbranched actin filaments (Yamda et al., 2013). Formins are found across eukaryotic phyla, but the FMN2 subfamily is confined mainly to the metazoa. Interestingly, spires have the same phylogenetic distribution as the relatives of FMN2. This evolutionary confluence is nearly exact and includes the concomitant loss of both FMN2 and spire in nematode worms and the co-appearance of both genes outside the metazoan clades, in the same choanoflagellate species.

Soon after discovering its nucleation activity, we discovered that Drosophila spire binds directly to a FMN2 ortholog called cappuccino (Quinlan et al., 2007). The connection between FMN2 and spire turns out to be conserved in many other species, including mammals, and involves direct interaction of the globular Kinase-Inactive N-terminal Domain (KIND) of Spire

with the unstructured C-terminal ‘tail’ of FMN2, sometimes known as the Formin-Spire Interaction (FSI) motif. At the level of molecular mechanism, the synergy between Spire and Formins is believed to depend on Spire as the nucleator and FMN2 as the polymerase, where Spire nucleates and then hands the actin nucleus off to FMN2 for elongation (Montaville et al., 2016). A significant implication of the physical and phylogenetic connections between spire and FMN2 is that the DNA repair mechanism they support cannot be universal but must be limited more or less to metazoans.

In a large proteomic screen, Matsuoka et al. reported the phosphorylation of FMN2 with the activation of DNA damage response kinases, ATM and ATR (Matsuoka et al., 2007). The multiple phosphorylation sites are located in the N-terminal region, flanked by two nuclear localization sequences that we identified and verified. We find that upon DNA damage, FMN2 is translocated from the cytoplasm into the nucleus. It is unclear whether the DNA damage-induced phosphorylation plays a role in this nuclear translocation by revealing/activating the NLS or if the phosphorylation results in a change in FMN2 function. Another group also reports the nucleocytoplasmic trafficking of a cleaved version of FMN2 during hypoxia (Yamada et al., 2013), with the N-terminal region entering the nucleus and the nucleation-competent C-terminal FH1-FH2 domains remaining cytoplasmic.

We previously showed that nuclear actin filament formation after DNA damage is also dependent on both Spire isoforms, Spire1 and Spire2, as the loss of Spire1/2 results in the loss of nuclear actin filaments. A bioinformatic search found no NLSes in Spire1/2, but curiously, a proteomic study identified Spire2 at pH2AX sites (Aymard et al., 2017). How Spire1/2 translocates into the nucleus and its role in DNA damage-induced nuclear actin filament formation are unknown. Further bioinformatic queries across metazoans containing Spire and FMN2 resulted in the discovery of an NLS being present in Spire, if the FMN2 homologues did not contain an NLS. DNA repair is dependent on nuclear actin filament formation, which is contingent on FMN2’s ability to translocate into the nucleus. Schrank et al (2018) reported that it

is Arp2/3 and its regulator N-WASP, not FMN2, that plays a critical role in the homologous repair pathway where the knockdown of FMN2 did not result in a change in HR repair efficiency (Schrank et al., 2018). However, the I-SceI repair assays used to detect repair efficiency have low sensitivity for detecting changes in efficiency due to the low percentage of cells in the assay that are transfected with the I-SceI restriction enzyme plasmid to trigger the damage and repair readout. This is further weakened by cell cycle regulation of homology-directed repair, where HDR mostly occurs during the G2 and S phase of the cell cycle (Shibata, 2017). Therefore, the role of FMN2 in the DNA repair process cannot be discounted from results that rely on the I-SceI system, as knockdown of FMN2 not only results in more DSBs but also a greater and more persistent degree of DNA damage in comet assays and 53BP1 foci (Belin et al, 2015).

The Arp2/3 complex has long been characterized for its ability to form branched actin networks in the cytoplasm, where it plays a critical role in the dynamics of cell motility, phagocytosis, endocytosis, membrane trafficking, and cell signaling (Hinze et al., 2018; Steinbacher and Ebnet, 2018). Only recently has it been observed to be involved in nuclear processes such as DNA repair, where Arp2/3 reportedly colocalizes to double-stranded break sites with its activator, WASP, and play a role in homology-directed repair through its actin nucleating activity (Caridi et al., 2018; Schrank et al., 2018). We decided to gain more insight into the role of Arp2/3 in the DNA repair process through biochemical characterization to answer the question of whether Arp2/3 interacts directly or indirectly with the DNA that it assists in repairing. Additionally, we determined how Arp2/3 is binding the DNA by identifying the subunit responsible and confirmed that Arp2/3 plays a role in both homology-directed repair, as previously reported, and also non-homologous end joining repair.

2. RESULTS

2.1. Arp2/3 binds DNA

Given the actin nucleator Arp2/3's role in DNA repair and reported localization to sites of DNA damage, we asked whether Arp2/3 directly or indirectly interacts with DNA by assessing its ability to bind DNA. Preliminary experiments were done with porcine Arp2/3, with following experiments using Arp2/3 complex that was purified from *Acanthamoeba castellani* and from bovine thymus to determine whether Arp2/3 had DNA binding activity.

We performed electrophoretic mobility shift assays (EMSA) with different concentrations of Arp2/3 and different forms of DNA to detect and characterize Arp2/3 binding activity by band shifts observed with protein-DNA binding on non-denaturing 3% agarose gels (**Figure 1**).

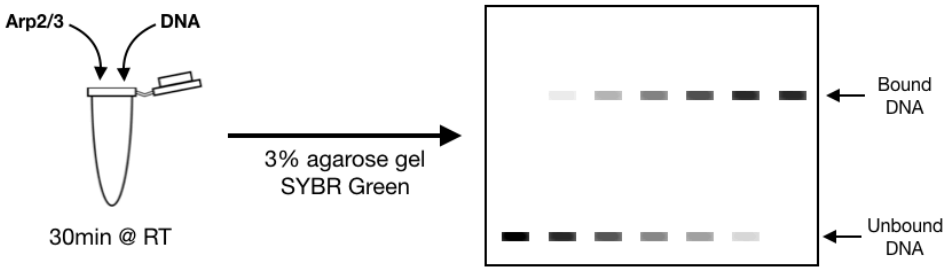

Figure 1. Electrophoretic mobility shift assay design. This schematic illustrates our EMSA setup to detect Arp2/3-DNA binding. Purified Arp2/3 was added to various oligos, incubated for 30min at room temperature before being run on an agarose gel, and stained with SYBR Green to detect DNA binding on a GelDoc Imager. The limit of detection in this assay is lower due to using SYBR Green versus radioactive-labeling.

Linear DNA and plasmid DNA were used to determine whether Arp2/3 bound preferentially or only to exposed DNA ends, as present in linear DNA and as seen with DNA double strand breaks, or whether Arp2/3 bound indiscriminately to DNA. Arp2/3 bound to both plasmid and linear DNA starting at the 250nM concentration in the EMSA, at which point the SYBR Green stained DNA shift could be detected (**Figure 2**).

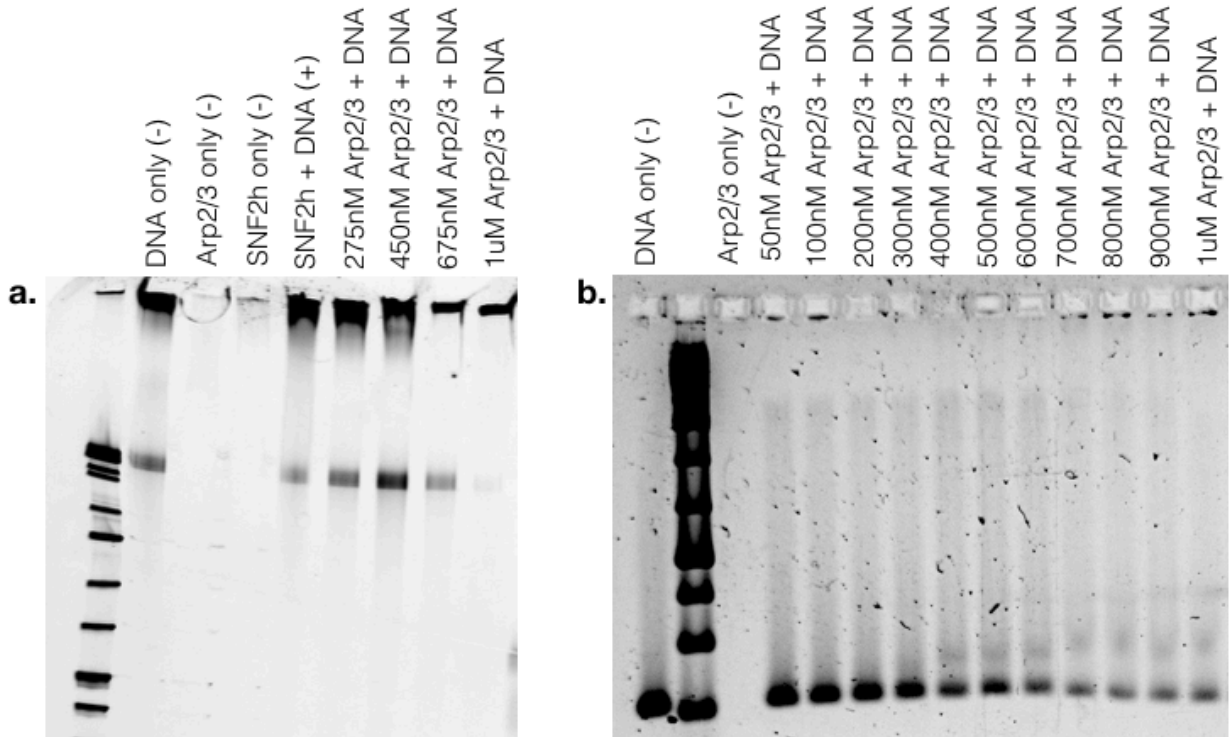

Figure 2. Arp2/3 binds to DNA. Arp2/3 bound both **a.** plasmid DNA at 4.5 kb and **b.** linearized DNA fragment at 270 bp. DNA concentration was kept consistent at 10nM while the amount of Arp2/3 increased. The size of Arp2/3 made it difficult to enter the 3% agarose gel, thus much of the Arp2/3 remained in the wells. A portion of the plasmid DNA was observed to remain in the wells likely due to size. However, binding was observed by the reduction of the DNA input in both cases. Irregularity with the 450nM Arp2/3 and plasmid DNA is likely due to pipetting error, as subsequent experiments showed consistent increased binding with increased Arp2/3. SNF2h, a chromatin-remodeling protein, used as a positive control.

We further characterized Arp2/3's DNA-binding activity by determining the parameters of this DNA-binding activity. DNA oligos of different lengths were used to establish whether a DNA length threshold was required for DNA-binding by EMSA. Arp2/3 binding persisted at every oligo length down to 20bp, with no stark differences between the different lengths tested (**Figure 3**).

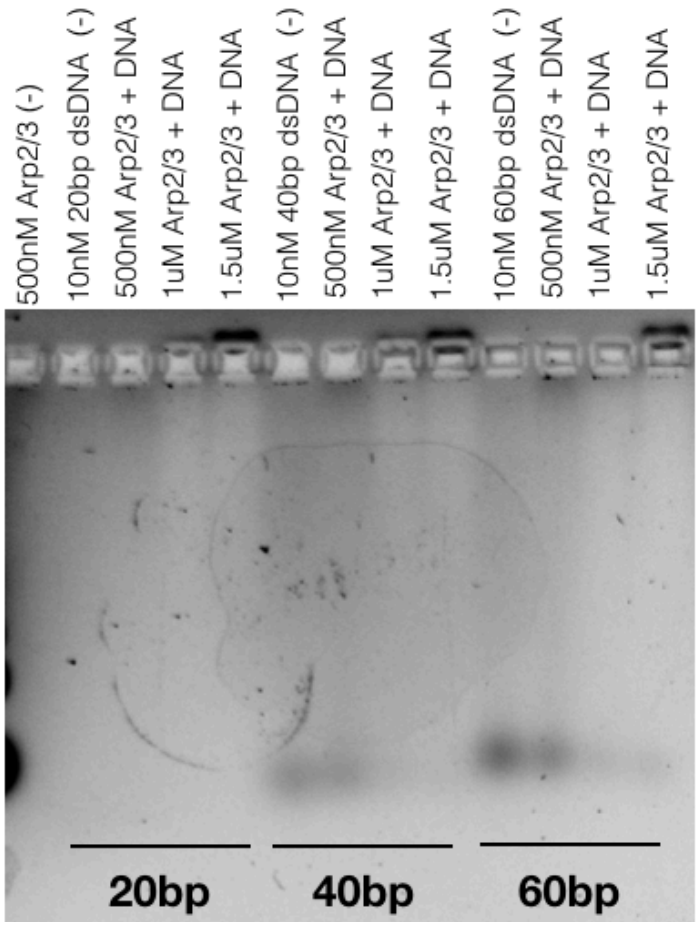

Figure 3. Arp2/3 binds to various lengths of DNA. EMSAs were done with different lengths of DNA to determine what the lower limit of binding was, GC-content was at around 50% for all oligos. DNA oligo concentration was kept at 10nM while Arp2/3 concentration was increased. The 20bp oligo was difficult to detect due to detection sensitivity. Previous experiment establishing binding with linearized DNA was with a 270bp fragment, while this experiment went down to 20bp with Arp2/3 still exhibiting DNA binding.

The homologous recombination DNA repair process produces single-stranded DNA during resectioning, where a 3' ssDNA is generated by endonucleases to invade the homologous DNA strand. Therefore, we wanted to test if Arp2/3 bound both ssDNA and dsDNA by performing an EMSA with ssDNA and dsDNA oligos and the Arp2/3 complex. Arp2/3 bound both dsDNA and ssDNA, with a preference for ssDNA (**Figure 4**), which will be further explored in the following sections.

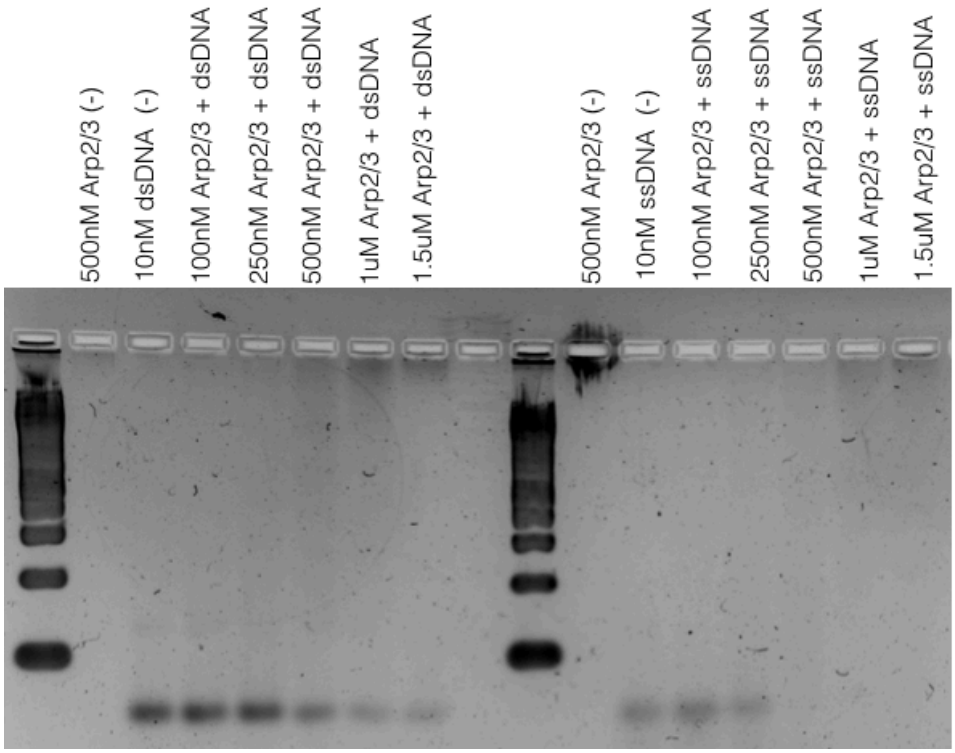

Figure 4. Arp2/3 preferentially binds to ssDNA. Either dsDNA or ssDNA oligos were added to Arp2/3 in EMSAs, where a preference for ssDNA was found. Although Arp2/3 binds both dsDNA and ssDNA, Arp2/3 showed stronger binding by the reduction in DNA input occurring at lower concentrations of Arp2/3 compared to Arp2/3 with dsDNA. The DNA shift is observed at 250nM Arp2/3 concentration for ssDNA, versus 500nM for dsDNA.

We next set out to measure the binding affinity of Arp2/3 for DNA by using fluorescence anisotropy, with reactions consisting of DNA oligos labeled at the 5'-end with 6-carboxyfluorescein and unlabeled Arp2/3. Binding of the labeled oligo by Arp2/3 results in a slowing down of the labeled oligo in solution, therefore resulting in an increase in anisotropy as measured by the fluorescence given off by the larger bound complex. Fluorescence anisotropy was used to produce a Kd for Arp2/3 with dsDNA but not ssDNA, as the ssDNA structure is too volatile for accurate measurements by fluorescence anisotropy. We found that Arp2/3 bound a 60mer dsDNA oligo with a Kd of 250nM, which is a binding affinity that is in lieu with other nuclear DNA-binding proteins (**Figure 5**).

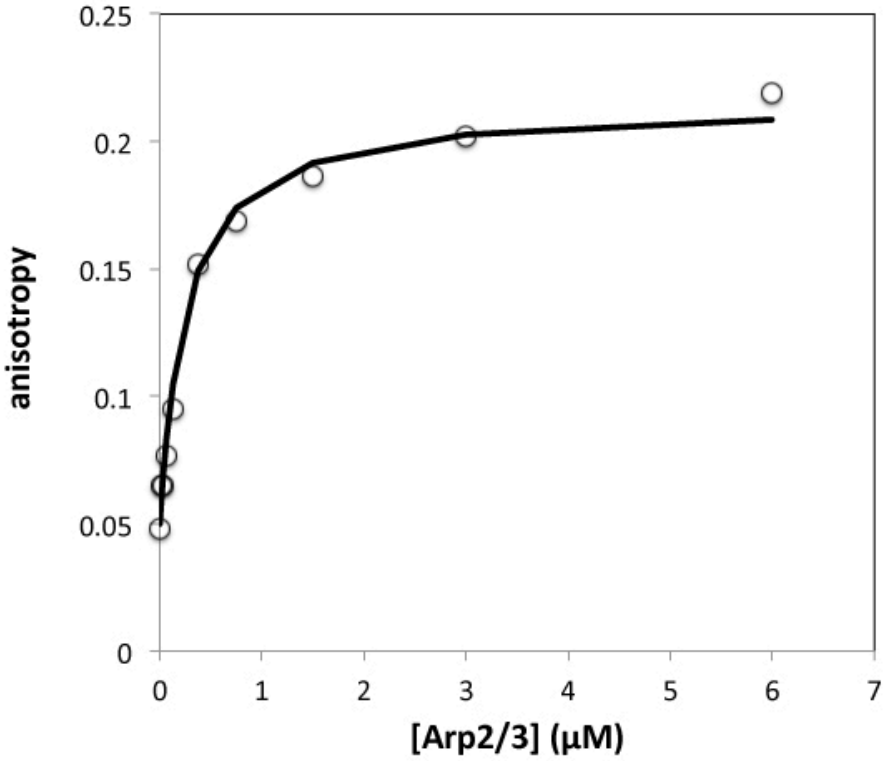

Figure 5. Arp2/3 binds to DNA with nanomolar affinity. Arp2/3 DNA binding affinity was measured by fluorescence anisotropy and yielded a respectable K_d of 250nM.

2.2. Arp2/3 DNA-binding activity is conserved across species

DNA repair occurs in all species to some degree, but there are nuances between species. For example, homology-directed recombination is the dominant repair pathway in yeast, whereas in mammals, non-homologous end-joining is the dominant repair pathway, with HDR being restricted to the G2 and S phases of the cell cycle (REF). Repair fidelity is lower with non-homologous end-joining, as the two broken ends are quickly joined together, sometimes resulting in the loss of base pairs that can lead to genetic mutations. We studied whether Arp2/3 across different species, ranging from unicellular to multicellular, would exhibit DNA-binding activity, indicating a potential role in DNA repair across species. We found that the DNA-binding activity of the Arp2/3 complex is conserved across species as Arp2/3 from A. castellani, bovine, and porcine are all able to bind DNA comparably, as Arp2/3 from various sources were used in our studies.

2.3. Arp2/3 preferentially binds ssDNA over dsDNA

We next looked to determine whether Arp2/3 binding was dependent on certain DNA conformations or motifs by using a DNA curtain system to study and visualize the nuances of Arp2/3 binding to DNA, where labeled DNA strands are arranged in a microfluidics flow chamber prior to labeled Arp2/3 flowing over the DNA to capture any binding events (**Figure 6**).

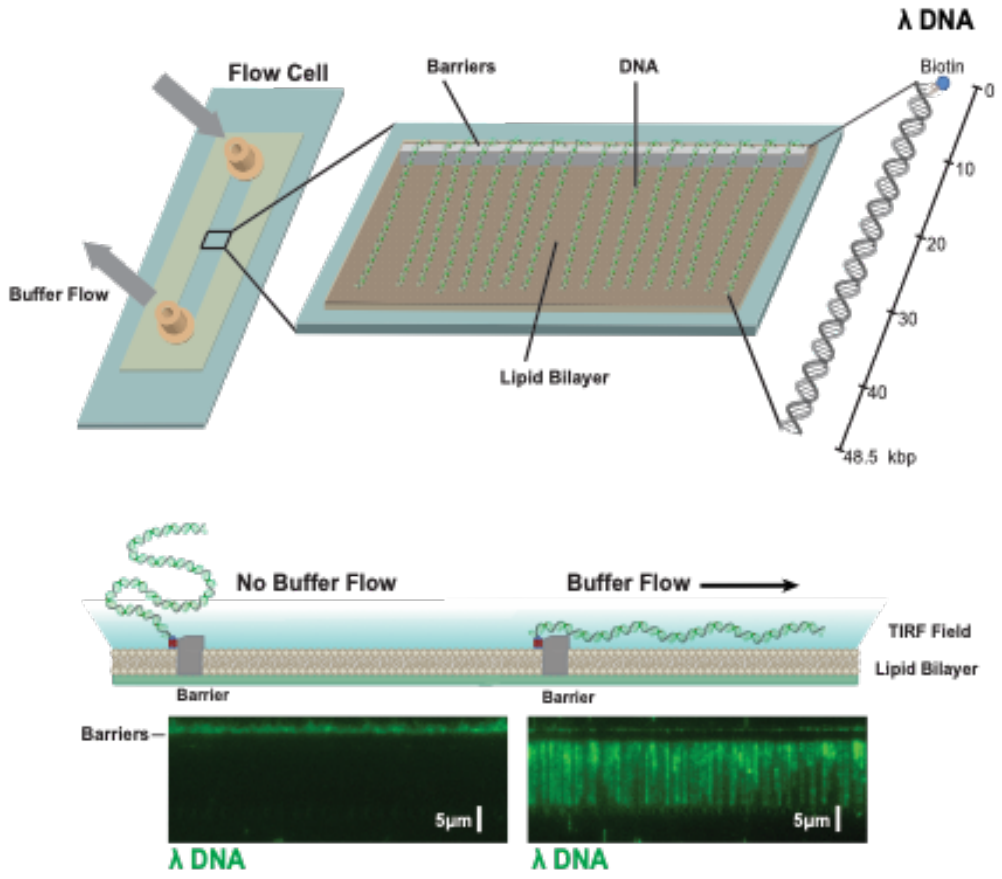

Figure 6. Arp2/3 DNA curtains design. In this experimental setup, fluorescently labeled lambda phage DNA is biotinylated and flowed over a lipid bilayer in a microfluidics flow chamber containing barriers that catch the biotin to produce an array of biotinylated DNA along the barrier that straighten out when flow is turned on. Arp2/3 that is labeled with a contrasting fluorophore is then added and incubated in the flow cell with the DNA curtains with flow off for 10min. Flow is turned on to wash away the unbound Arp2/3 and both the DNA curtain and Arp2/3 bound to DNA is visualized with TIRF.

Lambda DNA was used to determine whether Arp2/3 had a preference for certain DNA conformations or sequences, due to the sequence and structure of lambda DNA being known and well-characterized. We observed Arp2/3 binding consistently to the AT-rich region of lambda DNA on the DNA curtains, and also observed binding across multiple DNA strands in a "sashing" manner (**Figure 7**). Increasing the amount of Arp2/3 in the flow chamber eventually led to binding outside of the AT-rich region and resulted in full saturation on the DNA curtains.

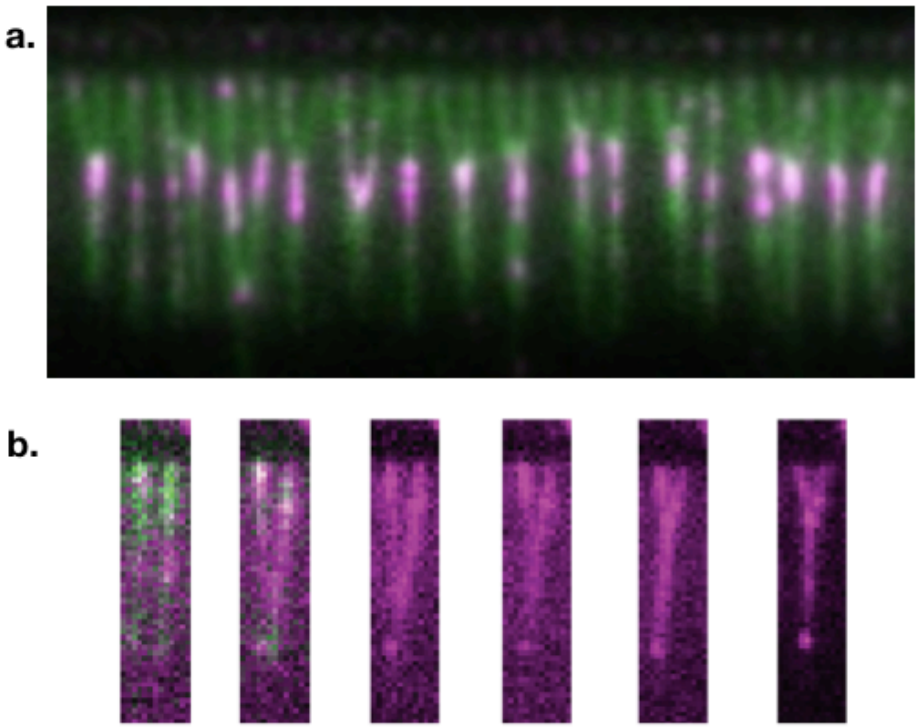

Figure 7. Arp2/3 binds multiple strands of DNA at a time. Addition of Alexa 506-labeled Arp2/3 (magenta) to lambda phage DNA curtains, labeled with Alexa 488 (green), showed **a.** consistent Arp2/3 association in the same DNA range throughout the curtains. A case for multivalent interactions could be made as multiple DNA strands were found to associate with each other where the Arp2/3 bound. **b.** Increasing the amount of Arp2/3 in the chamber eventually led to saturation of the entire DNA strand with Arp2/3.

An explanation for why Arp2/3 preferentially binds to the AT-rich region could be that AT-rich sequences exhibit a lower melting temperature due to the base stacking energies being lower, indicating that Arp2/3 may have a preference for ssDNA over dsDNA. To confirm that Arp2/3 was indeed binding to the AT-rich region, labeled dead Cas9 was used to mark the

region through guide RNAs designed to complement the sequences flanking the AT-rich region. Curiously, in the attempt to identify the AT-rich binding preference by using dead Cas9 (dCas9), Arp2/3 was found to preferentially colocalize with the dCas9. dCas9 localized to specific regions of the lambda phage DNA curtain by guide RNAs flanking the AT-rich region of interest. dCas9 was incubated with the lambda DNA curtain to establish the frame of reference prior to addition of Arp2/3. Addition of Arp2/3 resulted in the colocalization of Arp2/3 to the dCas9 binding sites.

2.4. Arp2/3 binds DNA through the p41 subunit

After establishing that Arp2/3 binds all forms of DNA, with a potential preference for some, we sought to determine how Arp2/3 is binding DNA by identifying the subunits that are responsible for DNA-binding activity. We hypothesized that the negative charge of DNA is likely interacting with the positively charged patches of Arp2/3, of which there are two belonging to two separate subunits, p41 and p21 (**Figure 8**).

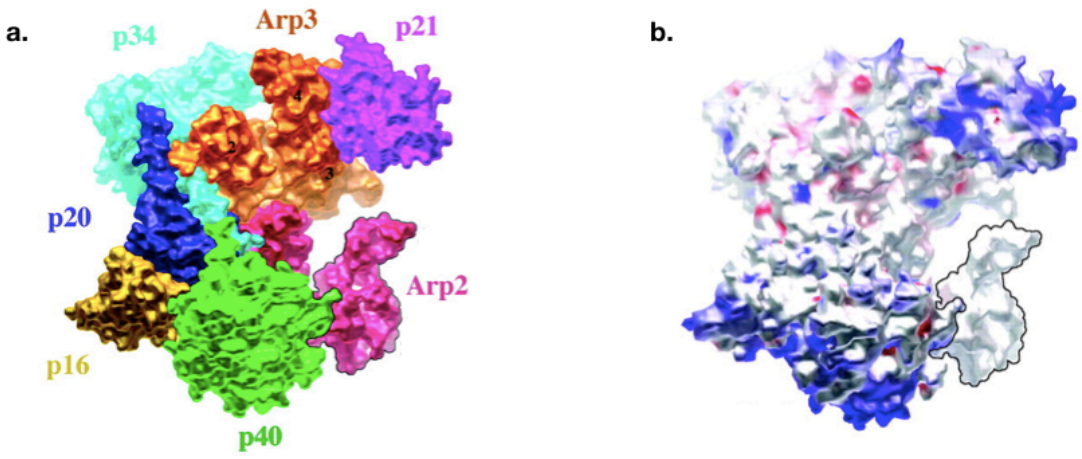

Figure 8. Arp2/3 contains two positively charged subunits. Arp2/3 consists of **a.** seven subunits, with two of these subunits being positively charged and likely to interact with negatively charged DNA. **b.** The two subunits, p41 and p21, sit on opposite sides of the complex and their positive charge is denoted by blue shading. The p21 subunit is known to interact with WASP VCA to enable activation of the Arp2/3 complex, while the functions of the p41 subunit are not completely understood.

To identify the Arp2/3 subunit(s) involved in DNA binding, we used psoralen UV-crosslinking to covalently link the DNA to Arp2/3 protein. Psoralen is a crosslinker moiety that

intercalates into pyrimidines of nucleic acids and primary amines of proteins upon long wave UV irradiation. The psoralen-labeled DNA is also capable of effectively conjugating primary amines of close enough proximity to the DNA, resulting in a covalently bound DNA-protein complex that can be further studied. Crosslinked reactions were run on SDS-PAGE gels and Western Blots performed with antibodies against each Arp2/3 subunit to identify band shifts indicative of DNA binding (**Figure 9**).

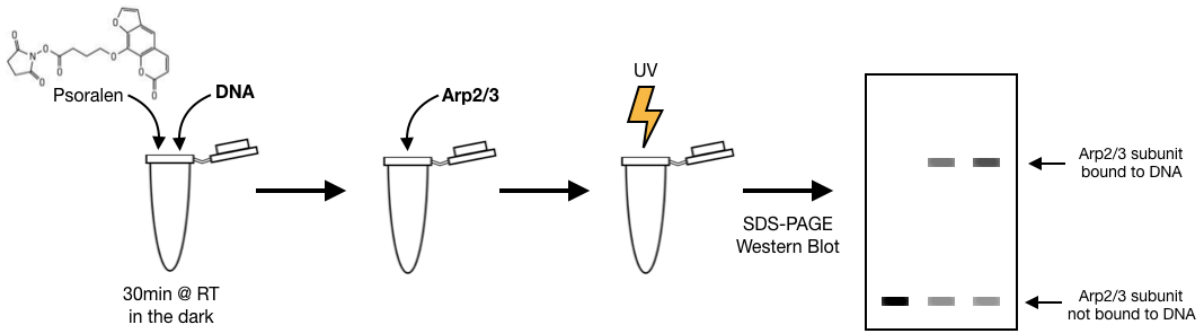

Figure 9. Arp2/3-DNA psoralen crosslinking design. In this schematic, psoralen is added to the DNA oligos in a preincubation step that allows for intercalation with pyrimidines. Post-incubation, the psoralen-DNA is added to the Arp2/3 in a binding reaction and incubated for 30min at room temperature before UV irradiation. UV irradiation activates the psoralen-DNA and results in covalent bond formation between the psoralen-DNA and protein. UV crosslinked reactions are then run on an SDS-PAGE gel for subunit separation and probed for each subunit by Western Blot using antibodies against individual subunits. A shift in bands between Arp2/3 alone and Arp2/3 with psoralen-DNA is indicative of DNA-binding through that Arp2/3 subunit.

No band shifts were detected for the p16, p20, p21, and p34 subunits, however, a novel band emerged when probing for p41 in the crosslinked Arp2/3 with DNA reaction versus Arp2/3 alone (**Figure 10**). Less specific higher molecular weight species were present for Arp2 and Arp3, indicating a potential role in DNA binding, however, their presence was not as compelling as the clear higher molecular weight band in p41. The lack of band shift for p21, which also contains a negatively charged patch, suggests that the DNA binding is not promiscuous in its binding to Arp2/3 and that p41 is the Arp2/3 subunit that the DNA is binding to.

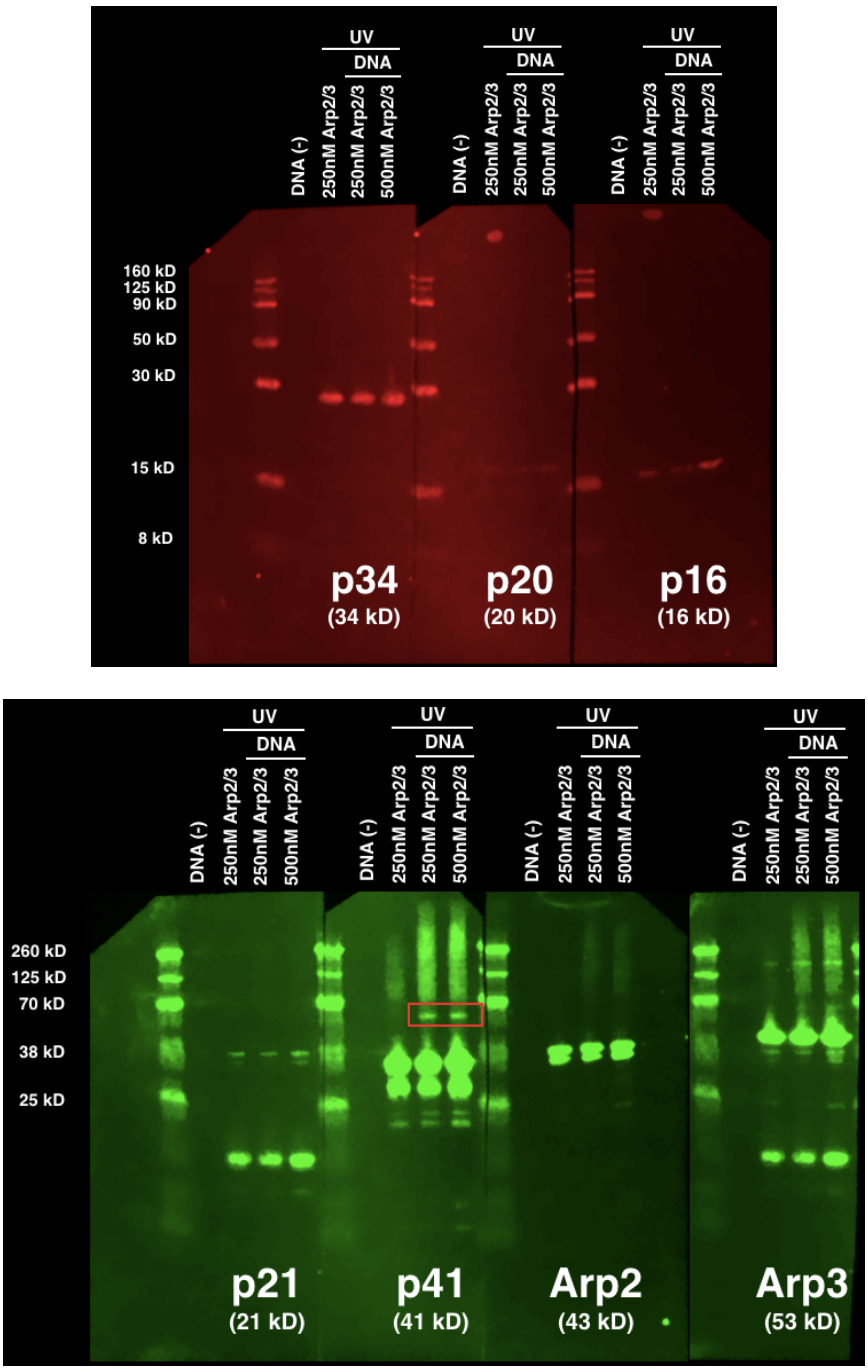

Figure 10. DNA binds to the p41 subunit of Arp2/3. A notable shift was observed with the p41 subunit after psoralen DNA-protein UV crosslinking compared to Arp2/3 alone, as noted with the red box. The appearance of this new band is indicative of an increase in molecular weight due to the Arp2/3 p41 subunit covalently binding psoralen-DNA. No other prominent band shifts were observed in other subunits, however, higher molecular weight smears appeared when probing for the Arp2 and Arp3 subunits. This shift occurs in the presence of both ssDNA and dsDNA.

The p41 subunit is responsible for Arp2/3 interaction with WASP family proteins, which activate Arp2/3 for actin nucleation. There are two isoforms of p41 in mammals, ARPC1A and ARPC1B, that may serve different functions in the cell depending on cell type, with ARPC1B being primarily expressed in platelets and resulting in platelet abnormalities in patients with ARPC1B deficiency. The presence of one isoform over the other in the Arp2/3 complex has been shown to confer different levels of Arp2/3 activity, and the isoforms are not functionally interchangeable. To determine whether one or both p41 isoforms were involved in Arp2/3 DNA binding, antibodies against each isoform were used to probe crosslinked reactions (**Figure 11**).

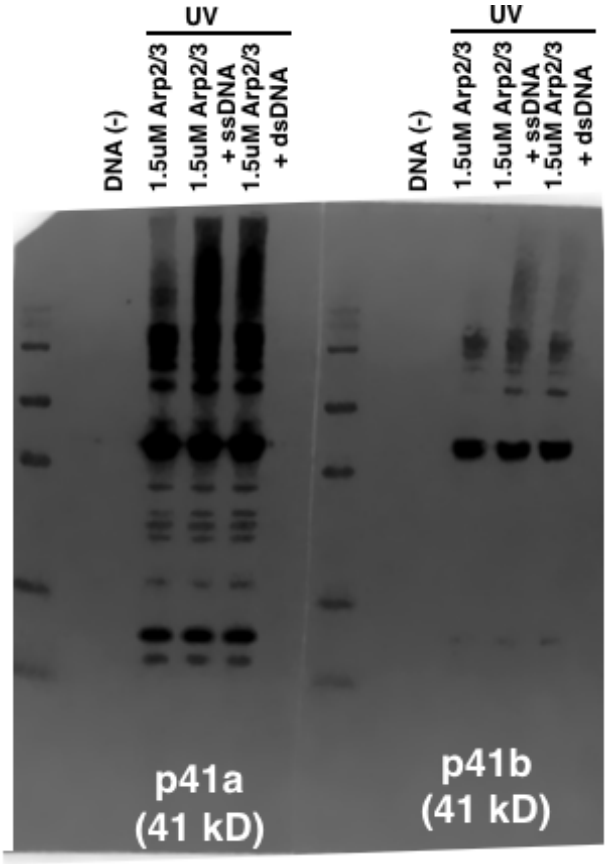

Figure 11. DNA interacts with the p41b isoform. Psoralen-DNA protein UV crosslinking and Western Blots were performed as before, however the antibodies used were p41 isoform-specific antibodies to determine which antibody, if not both, were capable of binding DNA. The p41 isoform-specific antibodies detected bands at around 41 kDa in the sample, indicating that both p41 isoforms were present. However, only p41b showed a strong band shift with the addition of psoralen-DNA to the Arp2/3, leading us to believe that the p41b is the one responsible for Arp2/3 DNA binding activity.

2.5. Arp2/3 DNA-binding does not affect its actin nucleation activity

Arp2/3 is an actin nucleator that is regulated by WASP proteins, which bind to Arp2/3 through the VCA domain to induce a conformational change that activates Arp2/3 for actin nucleation activity. Unlike other actin nucleators that shuttle into the nucleus upon DNA damage, we found that Arp2/3 is constitutively present in the nucleus. In order to determine if Arp2/3 is constitutively present in the nucleus or translocates into the nucleus upon DNA damage, HeLa cells were gamma-irradiated to induce DNA damage before nuclear fractionation to isolate the nucleus. Western Blots were done to detect the presence of Arp2/3 in the isolated nuclei by using Arp2 antibody. Arp2/3 was found to reside in the nucleus in both un-irradiated and irradiated cells, leading us to conclude that Arp2/3 is constitutively present in the nucleus.

Therefore, we investigated whether Arp2/3 DNA-binding activity is mutually exclusive of VCA-binding by a series of competition assays to determine whether the addition of VCA or DNA affects Arp2/3 binding to the other. We started by asking whether the VCA domain binds DNA, since the VCA interacts with Arp2/3 and if DNA bound VCA, then ostensibly, DNA-binding could sterically occlude VCA from also binding Arp2/3. Alternatively, VCA exhibiting DNA-binding activity could mean Arp2/3 and VCA both bind DNA at that interface, although it is unlikely due to Arp2/3 and VCA interactions in the cytoplasm. We found that VCA does not bind DNA in an EMSA where increasing amounts of VCA was added to DNA (**Figure 12**).

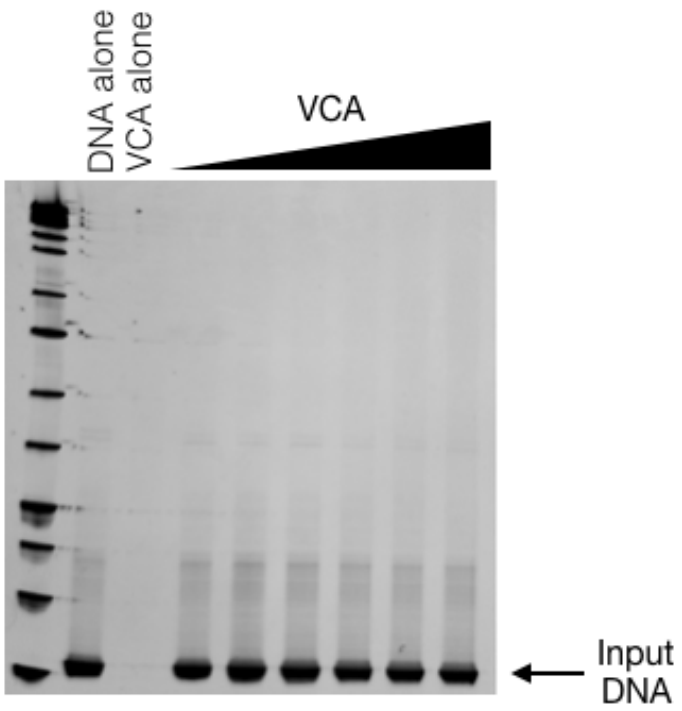

Figure 12. VCA does not bind DNA. EMSAs were performed with DNA oligos and increasing amounts of VCA to determine if VCA is capable of DNA-binding. There was no shift observed, indicating no DNA-binding activity from the VCA domain.

After determining that the VCA does not bind DNA, we asked whether Arp2/3 binding to DNA was mutually exclusive of its VCA binding ability. If Arp2/3 can only bind one or the other, then the implications would be that it is unable to nucleate actin while bound to DNA due to VCA being unable to activate it. And vice versa, if Arp2/3 cannot bind DNA while bound to VCA, then its DNA repair activity may be uncoupled from its actin nucleation activity. To test whether binding is mutually exclusive, titrating amounts of Arp2/3 and VCA were used in the presence of DNA to determine if addition of VCA would be capable of disrupting the binding interaction between Arp2/3 and DNA. We found that increasing amounts of VCA did not result in loss of Arp2/3 DNA-binding, indicating that the binding activities are mutually exclusive (**Figure 13**).

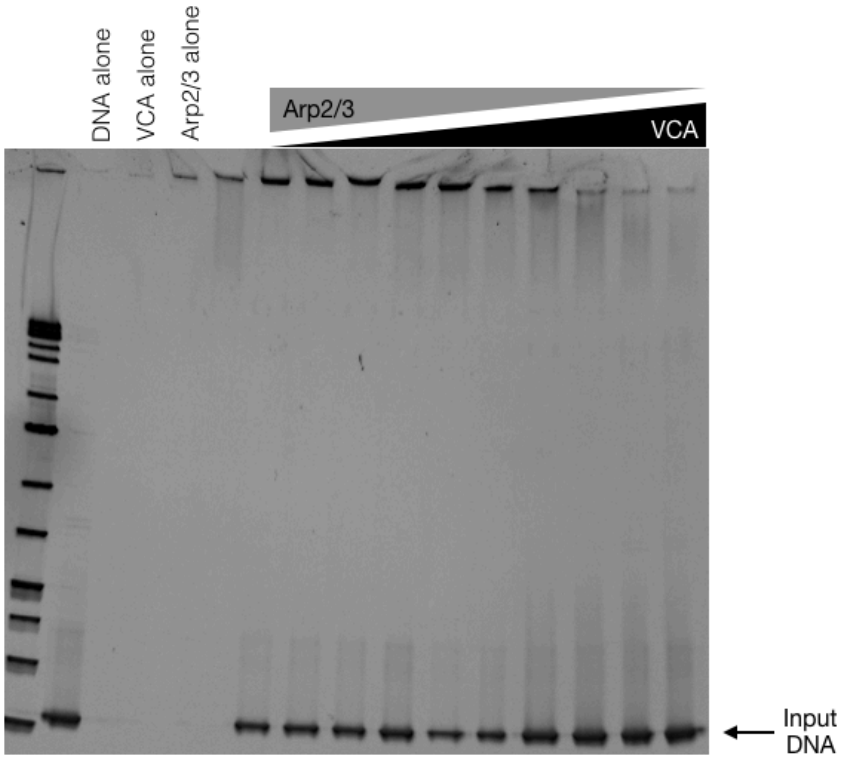

Figure 13. Arp2/3 and VCA binding is mutually exclusive of Arp2/3-DNA binding. DNA oligos were incubated with titrating amounts of Arp2/3 and VCA to determine if there was any competition for Arp2/3 binding between VCA and DNA. The DNA input was observed to decrease and shift upward with an increase in molecular weight in the presence of Arp2/3, despite the added presence of VCA.

To study whether DNA binding by Arp2/3 affects actin nucleation activity, we performed pyrene assays with Arp2/3 and VCA in the presence of DNA. Pyrene assays are used to measure actin nucleation and elongation in bulk by labeling actin monomers with pyrene, which is a fluorophore that can be introduced onto an existing cysteine in actin. In solution, pyrene actin monomers produce relatively little light scattering, but upon actin polymerization, there is an increase in light scattering due to the pyrene actin monomers organizing into higher molecular weight structures that increase fluorescence intensity that can be observed over time. With the addition of DNA, we observed that there was no significant change Arp2/3 with VCA's ability to nucleate actin, as the pyrene actin fluorescence curves were no different with or without DNA (**Figure 14**).

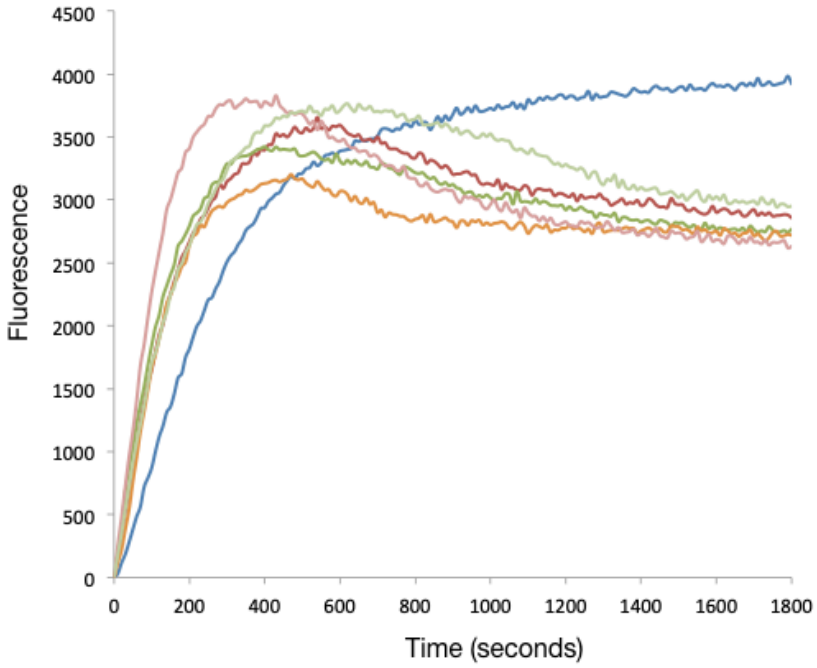

Figure 14. Arp2/3 DNA binding activity does not affect actin nucleation activity. Actin assembly was assessed with a pyrene assay, where actin monomers are labeled with pyrene and increase in fluorescence upon polymerization. Pyrene assays were performed with VCA-activated Arp2/3 nucleating the actin assembly in the presence or absence of DNA. The amount of DNA increased from 25ng to 500ng in the reaction series. Actin nucleation occurred without much inhibition even in the presence of DNA, indicating that Arp2/3 DNA-binding activity does not affect its ability to nucleate actin.

2.6. Arp2/3 plays a role in non-homologous end joining DNA repair

Arp2/3 was observed to play a role in promoting homologous recombination DNA repair, but not in non-homologous end-joining repair in I-SceI DNA repair assays. Briefly, cells are stably transfected with plasmids containing GFP sequences disrupted by I-SceI cut sequences that restore GFP activity by NHEJ or HR repair, and then transfected with a plasmid for expression of the rare restriction enzyme, I-SceI. Repair efficiency is determined by the percentage of GFP-positive cells, indicating a successful repair event. Although useful in detecting a variety of repair events, the variability introduced with multiple transfections could result in the underrepresentation of repairs, given that the GFP readout is typically <5% of cells across conditions (Vitor et al., 2020). We used the more robust class-switch recombination (CSR) assay to detect NHEJ. CSR in B-cells is facilitated by NHEJ repair to generate various

immunoglobulin classes and induction of CSR is well understood and much more feasible. We stimulated CSR in mouse CH12 cells with chemical inhibition of Arp2/3 to induce CSR from IgM to IgA and measured the efficiency of this class switching by flow cytometry to determine the ratio of IgM to IgA (**Figure 15**).

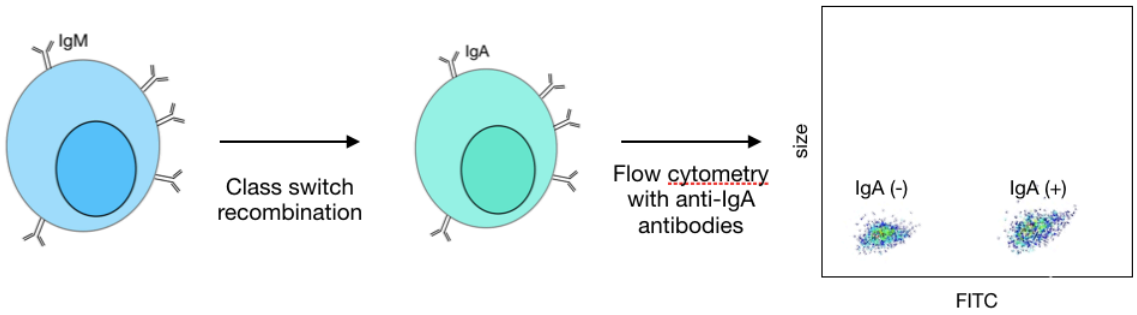

Figure 15. Class switch recombination assay design. In this schematic, the class switch recombination assay using CH12 cells is illustrated as a method for assessing non-homologous end joining repair efficiency. Immunoglobulin class switch recombination in B-cells occurs with the rearrangement of VDJ genetic fragments, which is facilitated NHEJ. In this assay, class switch is induced by addition of IL-4, anti-CD40 antibody, and TGF-beta to induce the immunoglobulin class switch from IgM to IgA. Efficient NHEJ repair allows for a greater degree of class switch recombination to occur, which is then read out by labeling the cell surface immunoglobulins and detection by flow cytometry.

First, we established that treatment with CK-666, a drug that inhibits Arp2/3 activity, has an effect on DNA repair. We irradiated CH12 cells with 5-gamma rays with and without CK-666 and performed comet assays on the cells at set time points after irradiation to observe DNA damage and repair efficiency. We found that CK-666-treated cells demonstrated a delay in DNA repair, as comet tails remained intact versus untreated cells over time, indicating that the damaged DNA had not been repaired yet (**Figure 16**).

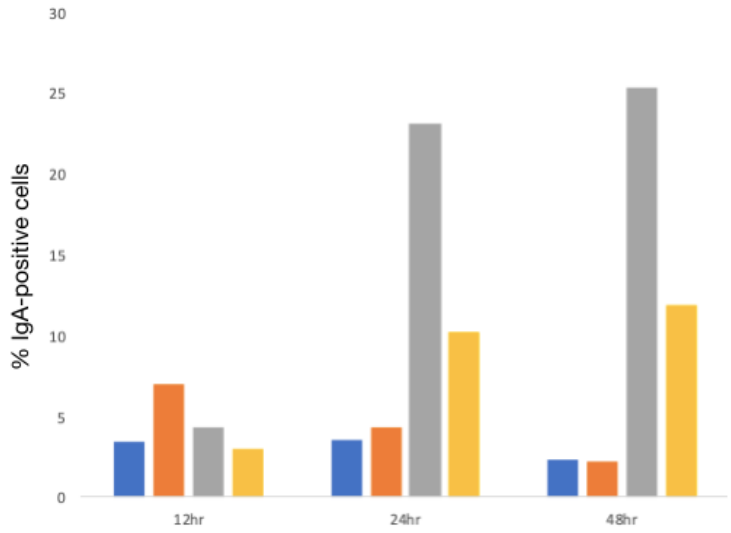

Figure 16. CK-666 treatment impairs NHEJ. Class switch recombination was done in the absence or presence of CK-666 to inhibit Arp2/3 activity prior to gamma irradiation to induce DNA. Samples were collected and processed at intervals of 12hr, 24hr, and 48hr post-damage to assess NHEJ efficiency. Cells that were treated with CK-666 exhibited a significant decrease in class switching efficiency, as seen by the reduced number of cells of the IgA positive cells. Blue indicates untreated cells and no CSR, orange is CK-666 treated with CSR, gray is untreated with CSR, and yellow is CK-666 with CSR.

2.7. Further evidence denoting the role of nuclear actin filaments and actin regulators in the DNA repair process.

In addition to Arp2/3 playing a role in DNA repair, we previously established a role for Formin2 and nuclear actin filaments. Both Arp2/3 and Formin2 are actin nucleators, albeit with different modalities, as Arp2/3 forms branched actin filaments while FMN2 is an actin nucleator that forms straight processive filaments. Additionally, both are heavily regulated, with Arp2/3 needing activation by interaction with a VCA domain and FMN2 being in an autoinhibited conformation prior to functioning as an actin filament elongator. The involvement of both known actin nucleators and previous studies implicate a role for nuclear actin filaments in DNA damage. To explore this, we wanted to establish an increase in DNA damage-induced nuclear actin filaments through quantitative phalloidin staining, which is a cytotoxin that intercalates and stabilizes actin filaments. Previous works observed the appearance of nuclear actin filaments after DNA damage using nuclear actin filament-specific probes, however, there are many

caveats with the known probes ranging from cytotoxicity to non-specificity to the probes themselves inducing actin nucleation (Belin et al., 2014; Du et al., 2015). By staining with fluorescently labeled phalloidin before and after inducing DNA damage, we found that there is an increase in nuclear actin polymerization after DNA damage based on the nuclear phalloidin signal (**Figure 17**).

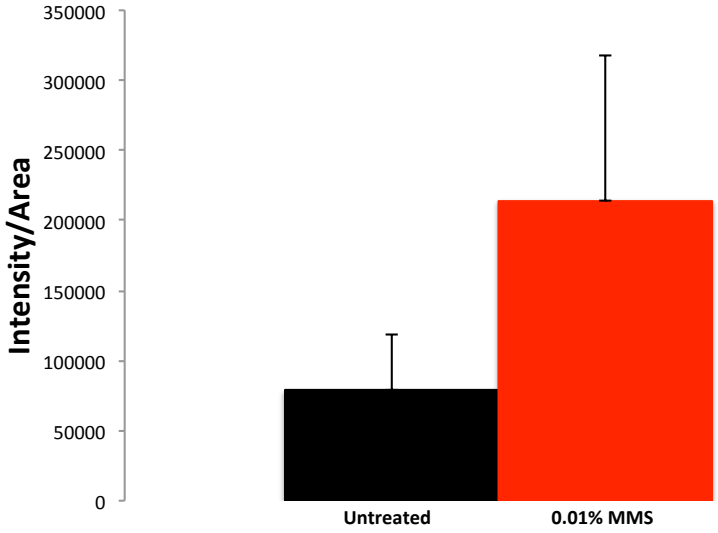

Figure 17. Increase in nuclear actin observed after DNA damage. HeLa cells were subjected to 0.01% MMS treatment for 1 hour to induce widespread DNA damage prior to fixation and quantitative phalloidin staining to determine if there is an increase in nuclear actin filaments after DNA damage. Phalloidin intercalates into actin filaments to stabilize and prevent depolymerization. The fluorescent phalloidin signal from the nuclei of DNA damaged cells was compared to untreated cells, with the results showing a significant signal increase in 0.01% MMS treated cells.

Previous studies in the lab showed that loss of FMN2 and the nuclear actin transporter IPO9 resulted in a greater number of 53BP1 foci after DNA damage with 0.01% MMS and was also linked to nuclear actin filament formation (Belin et al., 2015; Dopie et al., 2012). We delved deeper into characterizing the loss of FMN2 and IPO9 and their effects on DNA repair by assessing whether the increased DNA damage occurs due to a temporal delay in DNA repair that results in accumulation of DNA breaks or whether there is an overall increase in DNA repair. We studied this by performing Comet assays with WT and FMN2 and IPO9 knockdown cells, which look at the degree of DNA damage based on the amount of broken DNA that leaks

out of the nucleus. We observed greater levels of basal DNA damage in FMN2 KD cells, indicating that loss of FMN2 may impair the cell's ability to repair its DNA without apparent insult (**Figure 18**).

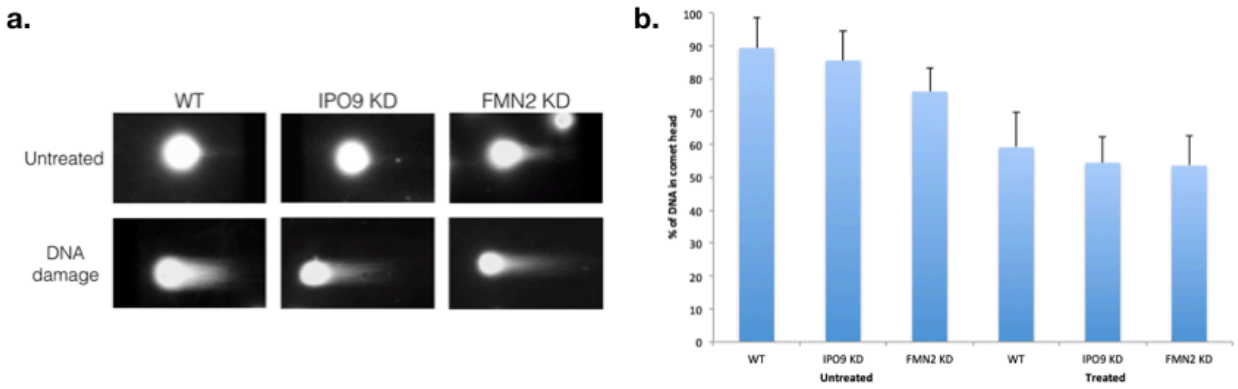

Figure 18. Loss of FMN2 results in higher basal levels of DNA damage. FMN2 and IPO9 knockdowns were generated by shRNAs as previously described in HeLa cells to compare the effects of the actin nucleator FMN2 and the nuclear actin importer IPO9 on DNA repair. Comet assays were performed by embedding cells in agarose prior to lysis to remove the cell membrane while keeping the nuclear membrane intact. Gel electrophoresis was then run on the samples, causing the nuclei to migrate toward the positive electrode due to the negatively charged DNA-containing nuclei. Samples are then stained with SYBR Gold to visualize the DNA, wherein healthy intact DNA migrates as a sphere while damaged DNA leaks out of the nuclear pores to create a comet tail effect. This initial assessment of basal DNA damage levels by performing comet assays on untreated WT and KD cells found that loss of FMN2 resulted in higher basal levels of DNA damage over WT cells, as indicated by the **a.** larger comet tails seen in FMN2 KD cells and **b.** quantification of these comet tails in bulk, where less DNA in the comet head indicates more broken DNA.

After establishing that FMN2 KD cells have increased DNA damage, we wanted to determine to what degree loss of FMN2 affected the DNA repair process. This was done by performing a time course study using the comet assay and inducing DNA damage with 1uM Bleocin, which induces both sequence-specific single stranded and double stranded breaks through the production of free radicals. Samples were taken periodically post-DNA damage and compared to WT cells that also underwent Bleocin treatment to determine whether the degree and timing of DNA repair was affected by loss of FMN2. We observed that in cells with FMN2 knocked down, we found that the comet tails indicative of DNA damage persisted for up to 48 hours before they were resolved in a manner that made them comparable to WT cells (**Figure**

19). Despite IPO9 not having a significant effect on baseline DNA damage, we included IPO9 in this study as well, and found that it also resulted in greater levels of DNA damage after 24hr.

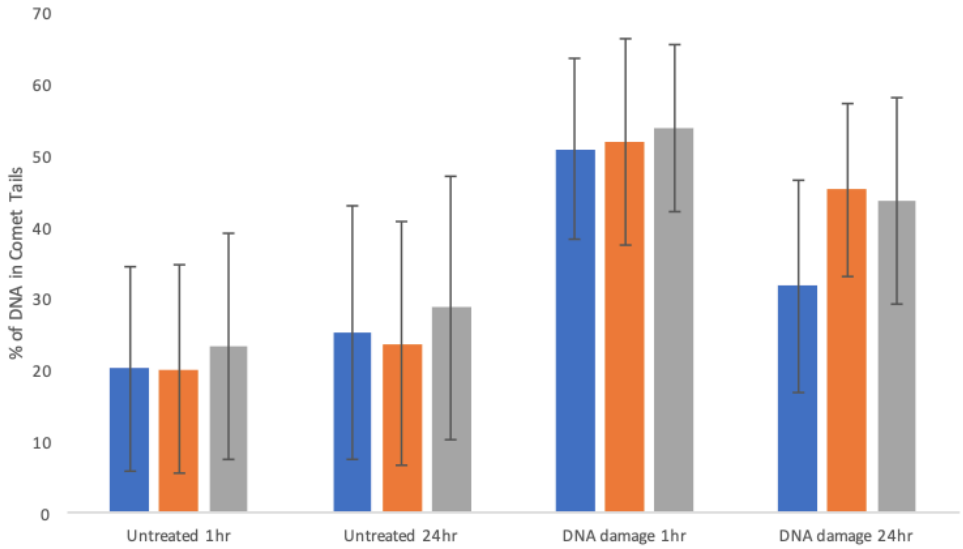

Figure 19. Loss of FMN2 delays DNA repair after insult. Using comet assays to assess DNA damage, we induced DNA damage by 1uM Bleocin and performed a time course experiment to assess DNA damage at 1hr and 24hr post-insult. We found that loss of FMN2 delayed DNA repair for up to 48hrs, with damage levels eventually becoming comparable to WT cells at the 72hr time point (not shown). Blue indicates WT cells, orange IPO KD, and gray FMN2 KD.

With the delayed DNA damage, we asked whether this had an effect on DNA damaged cells and their viability with the loss of FMN2 or IPO9. We used TUNEL assay to assess whether cell viability was affected by detecting DNA fragmentation that is characteristic of apoptotic cells. DNA damage was induced with two different DNA damaging agents, 1uM Bleocin and 0.01% MMS, which is a DNA alkylating agent that modifies guanine and adenine to produce base mispairing and replication blocks. MMS was used due to previous studies in the lab using it to induce DNA damage, but its nonspecific activity and toxicity due to ROS production resulted in us replacing it with Bleocin. Loss of IPO9 for nuclear actin transport results in delayed DNA repair but did not have an effect on cell viability. Despite an increase in basal DNA damage and delay in DNA repair with the loss of FMN2, loss of FMN2 does not appear to affect cell viability after DNA damage (**Figure 20**). This is supported by the fact that FMN2 KD cells do not exhibit abnormal growth or lethality when produced.

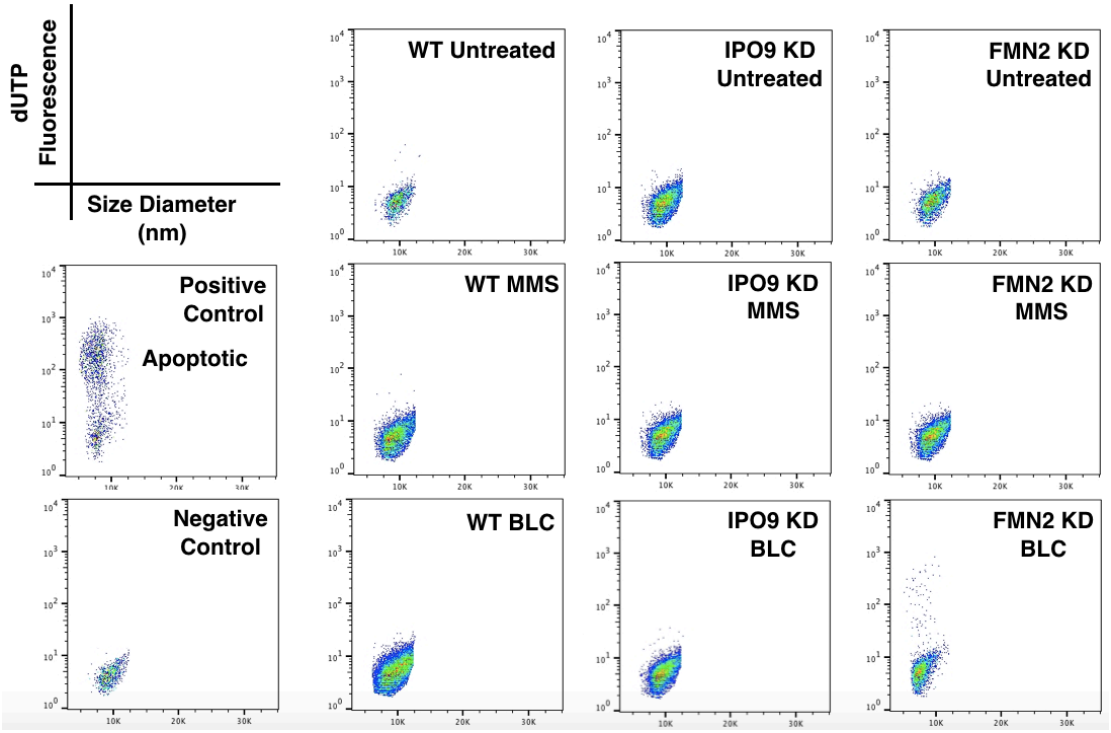

Figure 20. Loss of FMN2 does not affect cell viability after DNA damage. TUNEL assay was performed on WT, IPO9 knockdown, and FMN2 knockdown cells after DNA damage induction with either 0.01% MMS or 1uM Bleocin (BLC) to determine if there was a loss in cell viability due to the loss of FMN2. In the TUNEL assay, cells are fixed and then TdT enzyme and FITC-dUTP are added to the fixed cells to allow FITC-dUTP to incorporate into fragmented DNA that occurs during DNA damage and apoptosis. If cells are healthy and viable, then there is no incorporation of FITC-dUTP due to the DNA being supercoiled with no route of insertion. Apoptosis is detected by the fluorescent signal given off by the FITC-dUTP that incorporates in the DNA by flow cytometry.

3. DISCUSSION

DNA double strand breaks (DSB) are the most detrimental type of DNA lesion that occur, and if left unrepaired, jeopardize the genomic integrity and vitality of a cell. A successful DNA damage response requires the cell to sense the DSB, process it for repair, and then either repair or bypass it. Our studies provide additional support for the role of actin nucleators and actin filaments in the DNA repair process by demonstrating that the branched actin nucleator Arp2/3 binds directly to DNA and is important for non-homologous end joining. Its role in NHEJ is a novel discovery in that previous studies only showed its involvement in homology directed repair, while our studies suggest that it is involved in both of the major DSB repair pathways in mammalian cells.

We have shown that Arp2/3 binds DNA in both bulk solutions with the EMSAs and on a single molecule level with the DNA curtains. The binding to AT-rich regions and to the dCas9 appears to point to a preference for ssDNA, or at least to a D-loop conformation that reveals ssDNA. Earlier EMSA results showed that Arp2/3 bound both ssDNA and dsDNA, however, it was not clearly indicative of whether Arp2/3 exhibited a preference for ssDNA or dsDNA based on those results. A preference for ssDNA would place Arp2/3 at the DSB ends, where ssDNA is present in both homologous recombination (HR) and non-homologous end joining repair (NHEJ) processes. In homologous recombination, long regions of ssDNA are produced during resectioning by endonucleases processing the broken ends for strand invasion, while NHEJ short ssDNA regions are present at the break ends for microhomology driven repair (Liu and Huang, 2016).

The Arp2/3 p41 subunit was identified as the binding site for DNA, with one specific isoform showing some preference for DNA over the other. Future studies include identifying the specific binding site using aryl azide crosslinking and mass spectrometry to covalently bind Arp2/3 to the DNA in a manner independent of amine or pyrimidine groups, and mass spectrometry would identify the residues protected by the DNA binding during protease digest.

With the binding residues identified, further studies can be conducted through mutagenesis to ablate the binding activity and see those effects in vivo.

A caveat of studying actin and actin regulators in the nucleus is their ubiquitous nature that results in them being found throughout the cell. Perturbations that are nucleus specific would greatly advance the field by isolating the role of actin filaments and its regulators to the nucleus. This can be achieved by adding a nuclear localization signal to mutagenized actin regulators, therefore sequestering the majority of these modified activities to the nucleus. A dominant-negative Arp2/3 with an NLS could flood the nucleus with Arp2/3 that is unable to nucleate actin while maintaining Arp2/3 actin nucleation activity in the cytoplasm. Similarly, a mutagenized Arp2/3 that can no longer bind DNA could also be tagged with an NLS. Future studies will have to focus on nucleus-specific perturbations, which could involve simply using an NLS tag on actin regulators or the invention of new tools.

The emergence of Formin2 and Spire in metazoans lends to speculation that as organisms evolved in complexity, so did their mechanisms for DNA repair. Along with increased complexity and function, multicellular organisms encounter a multitude of challenges that free-living unicellular organisms do not. Cellular migration through tissue during multicellular processes such as embryogenesis, oogenesis, and the immune response, subject individual cells to the mechanical stresses of multicellularity. Cells must squeeze through collagen matrices and between neighboring cells in response to signaled migration, and recent studies have shown that cell migration can cause mammalian nuclear envelope rupture, which results in DNA damage (Thiem et al., 2016). The evolution of multicellular complexity not only increased the number of processes an organism performs and the specificity of cellular/tissue roles, but also increased the target size for DNA damage. Damage to one or too many cells compromises the entire organism, thus, a need for more sophisticated DNA repair methods evolved with multicellularity.

The study showing that FMN2 KD resulted in greater basal DNA damage indicates that it may be implicated in NHEJ, which occurs more frequently and is used to patch up most DNA damage events in mammals. The role of FMN2 in NHEJ and HR was refuted in a previous study, however, those studies did not convincingly show that FMN2 was not involved due to their use of the I-SceI assay. Future work will revisit the role of FMN2 in NHEJ using the class switch recombination assay used in this study.

The role of nuclear actin filaments in DNA damage remains unknown, but the evidence of actin nucleators being involved in this repair process points to actin polymers versus actin monomers being of importance. Below are three models where nuclear actin filaments play a potential role and future studies will hopefully determine which of this models or possible other ones are correct in explaining the role of nuclear actin filaments in DNA damage repair.

Model I: Nuclear actin filaments act as a scaffold for DNA repair factors. Andrin et al. showed that many DNA repair factors bind to filamentous actin *in vitro*, and postulate that nuclear actin filaments serve as a scaffold for DNA repair factors (Andrin et al., 2012). In particular, Ku70/80 was found to interact directly with filamentous actin *in vitro*, and the loss of actin polymerization in the nucleus resulted in the loss of DNA damage repair. The Ku70/80 heterodimer is involved in the stabilization of DSB ends in NHEJ repair, and thus could be using nuclear actin filaments as a scaffold to stabilize DSB ends and recruit later stage DNA repair factors. Alternatively, nuclear actin filaments could function as a scaffold to keep certain nuclear components away from the site of damage.

Model II: Nuclear actin filaments facilitate the clustering of DNA repair sites. DNA repair sites are an established phenomenon in *S. cerevisae* during HR repair; damaged DNA is recruited to DNA repair foci consisting of DNA repair factors (Shibata, 2017). The formation of these DNA repair factories is triggered upon detection of a DSB and is disassembled once DNA repair is completed. Long-range chromosomal movement is implicated in the recruitment of damaged foci to the repair factories, however there are still inconsistent accounts on the range

of chromosomal movements in mammalian cells (Kapoor et al., 2013; Olave et al., 2001). We do not see the co-localization of nuclear actin filaments with the DSB marker, 53BP1, but this does not rule out the potential role of nuclear actin filaments in the formation of DNA repair foci or the transport to these repair sites.

Model III: Nuclear actin filaments function as a monomer sink to regulate nuclear actin concentrations. Actin monomers are necessary components of many nuclear complexes, including various chromatin remodelers, transcription factors, and ribonucleoproteins. In response to DNA damage, a cell activates or inactivates certain cellular processes, such as increasing transcription of certain genes while shutting down transcription others or relaxing the chromatin structure around the site of damage to allow for DNA repair. Increasing the actin monomer concentration in the nucleus increases RNA Polymerase II activity (Huet et al., 2012; Philimonenko et al., 2004; Yoo et al., 2007), while knockdown of the nuclear actin importer, Importin9, was shown to decrease RNAPII activity (Vartiainen et al., 2007).

4. MATERIALS AND METHODS

4.1. Acanthamoeba castellani Arp2/3 complex purification and labeling

Arp2/3 was prepared from Acanthamoeba castellini by the method of Dayel et al. (2001). Briefly, 15L of Acanthamoeba castellani were grown up, harvested and washed into 10mM Tris, pH 8.0 at 4°C, 100mM NaCl. The cells were ruptured by release from a Parr bomb equilibrated with nitrogen at 400 p.s.i. Lysate was cleared with centrifugation first at a low speed, 15 min, 4k rcf at 4°C; then at a higher speed, 2 hrs, 113k rcf at 4°C. After centrifugation, the top layer of lipids was removed by gentle aspiration, and the pellet discarded. The lysate was loaded onto a DEAE column, and the flow through collected. The flow through was then loaded onto an NWASP WWCA-Sepharose column, washed with 10mM Tris pH 8.0, 50mM NaCl, 0.1mM CaCl2, 0.2mM ATP, 1mM DTT, 15 ug/mL Benzamidine. The protein complex was eluted with 10mM Tris pH 8.0, 400mM MgCl2, 1mM DTT, and dialyzed into MonoS low buffer (10mM Tris pH 8.0, 0.5mM TCEP, 0.5mM MgCl2, 0.1mM ATP). The sample was loaded onto a MonoS column (GE Healthcare) and eluted with a 0-500mM NaCl gradient. Selected fractions were gel filtered using a Superdex 200 column (GE Healthcare) into 20mM HEPES pH 7.0, 0.5mM TCEP, 25mM KCl, 0.2mM MgCl2, 0.1mM ATP. Glycerol was added to 10% and the purified protein flash frozen and stored at -80°C.

The A. castellani Arp2/3 complex was labeled with succinimidyl ester dye derivatives (Alexa Fluor 568). Arp2/3 was diluted into 0.5mM TCEP, 25mM KCl, 100mM sodium bicarbonate pH 8.3, 0.2mM MgCl2, 0.1mM ATP. Alexa Fluor 568 NHS Ester (Invitrogen) was dissolved in DMSO and added to 4 times above the molar concentration of protein, and allowed to incubate for 30 min at room temperature and 30 min at 4C, stirring and protected from light. Reaction was quenched with 1.5M hydroxylamine pH 8.5 for 1hr on ice. Free label was removed by buffer exchanging into 20mM HEPES pH 7.0, 0.5mM TCEP, 25mM KCl, 0.2mM MgCl2, 0.1mM ATP and 10% glycerol over a Zeba column. The labeled protein was flash frozen and stored at -80°C.

4.2. Electrophoretic mobility shift assays

Protein binding to DNA was detected by electrophoretic mobility shift assays (Invitrogen EMSA kit). A. castellani Arp2/3, bovine, or porcine Arp2/3 and oligos (IDT) were mixed in 10ul reactions with 5X binding buffer (750mM KCl, 0.5mM dithiothreitol, 0.5mM EDTA, 50mM Tris pH 7.4) and incubated at room temperature for 30min. 6X EMSA gel-loading solution was added to each reaction at the end of the incubation period and mixed gently. DNA-protein complexes were separated by electrophoresis using a 3% agarose gel made with 0.5X TBE (89mM Tris base, 89mM boric acid, 1mM EDTA pH 8.0). Gels were stained with SYBR Green EMSA nucleic acid gel stain (10,000X) diluted in 0.5X TBE and incubated for 20min at room temperature with gentle agitation and protected from light. Gels were washed twice with ddH2O for 10 seconds before visualization on a BioRad GelDoc.

4.3. Light scattering assays

Right angle light scattering was conducted by manually mixing A. castellani Arp2/3 and DNA in a digital K2 fluorimeter (ISS, Champagne, IL) using an excitation wavelength of 320 nm.

4.4. DNA curtains

Labeled arp2/3 was injected into the flow cell and incubated in the flow cell for 15min, followed by a wash of 1-2 mL of Imaging Buffer.

100 nM 3x-FLAG-tagged dCas9 was reconstituted with 1 μM crRNA:tracrRNA targeting the desired region of λ-DNA by incubating for ~10 min at 37 °C in Reaction Buffer (20 mM Tris-HCl pH 7.5, 100 mM KCl, 5 mM MgCl2, 5% glycerol, 1 mM DTT). 10 nM dCas9:RNA was then incubated with λ-DNA (100 pM) for ~15 min at 37 °C in 40 mM Tris-HCl pH 7.5, 25 mM KCl, 1 mg mL−1 BSA, 1 mM MgCl2, and 1 mM DTT, before being diluted to 1 nM and injected into the flow cell. The flow cell was then washed with 3–5 mL of Imaging Buffer containing 40 mM Tris-HCl, 25 mM KCl, 1mg mL−1 BSA, 1 mM MgCl2, 1 mM DTT, 0.75 nM YOYO1 (Life Technologies), 0.8% glucose, and 0.2X glucose oxidase/catalase. Finally, 0.5 nM anti-FLAG

antibody-coated QDs were incubated in the flow cell for 5 min, followed by a wash of 1–2 mL of Imaging Buffer.

4.5. Arp2/3-DNA crosslinking and Western Blots

DNA-protein UV crosslinking was performed as previously described (Sasstry 1997). Briefly, NHS-Psoralen (Thermo Scientific) was added to DNA oligo and incubated in the dark at room temperature for 30min in Arp2/3 buffer (20 mM Tris pH 7.5, 25 mM KCl, 1 mM MgCl2, 1 mM DTT). Porcine Arp2/3 (Cytoskeleton) was then added to the “dark” reaction and the mixture incubated for 30min at room temperature. Samples were irradiated with a UV crosslinker (Spectrolinker XL-1000) by placing samples on ice 5cm away from UV light source and irradiating for 60min. Control samples were treated identically except that the preincubation with psoralen was omitted.

Western blotting was done with the LiCOR Odyssey to visualize shifts from DNA binding using the following antibodies: rb polyclonal anti-ARPC2 (LSBio, LS-C102803; dilution 1:???), rb polyclonal anti-ARPC4 (LSBio, LS-C134953; dilution 1:), rb polyclonal anti-ARPC5 (Novus Bio, NBP2-14878; dilution 1:), ms monoclonal anti-Arp3 (Santa Cruz, sc-48344; dilution 1:), ms monoclonal anti-Arp2 (Santa Cruz, sc-166103; dilution 1:), ms monoclonal anti-ARPC3 (Santa Cruz, sc-166630; dilution 1:), ms monoclonal anti-ARPC1 (Santa Cruz, sc-271342; dilution 1:). To detect ARPC1 isoforms, the following antibodies were used as previously described (Kahr et al. Nat Comms 2017): rb polyclonal anti-ARPC1A (Sigma-Aldrich, HPA004334; dilutions 1:), and rb polyclonal anti-ARPC1B (Sigma-Aldrich, HPA006550; dilution 1:). LiCOR secondaries were as follow: IRDye 680RD Goat anti-Rabbit IgG (LiCOr, 926-68071; dilution 1:10,000) and IRDye 800CW Goat anti-Mouse IgG (LiCOr, 926-32210; dilution 1:10,000).

4.6. CH12 cell culture and gamma irradiation

CH12F3 (CH12) cells were a generous gift from Dr. Schwer and were cultured at 37C and 5% CO2 in RPMI supplemented with 10% (vol/vol) FBS, 5% (vol/vol) NCTC-109 (ThermoFisher), 1x MEM-NEAA (ThermoFisher), 1mM sodium pyruvate (ThermoFisher), 50

U/mL penicillin/streptomycin (ThermoFisher), 50 uM 2-mercaptoethanol (Sigma), and 20mM HEPES pH 7.4.

Cells were irradiated with 5 gamma-rays using a Cesium irradiator.

4.7. Comet assays and analysis

DNA strand breaks in CH12 cells were evaluated using the Trevigen Comet AssayTM kit (Trevigen, 4250-200-03) according to the manufacturer's protocol. Briefly, cells were spun down, rinsed with cold PBS (Ca2+ and Mg2+ free), spun down again, and resuspended in PBS to a concentration of 1x10^5 cells/ml. A dilution of 1:10 was made of 5ul of cell sample into 50ul molten LMAgarose (1% low-melting agarose) kept at 37C, 50ul was immediately pipetted and spread onto the comet slides. Slides were incubated in the dark at 4C for 10 min to solidify the agarose disc and then transferred to pre-chilled lysis solution (2.5 M NaCl, 100 mM EDTA, 10 mM Tris-base, 1% sodium lauryl sarcosinate, 1% Triton X-100, pH 10) for overnight lysis at 4C. After lysis, slides were washed with chilled 1X Neutral Electrophoresis Buffer (100mM Tris, 300mM sodium acetate, pH 9.0) for 30 min. Slides were placed in a horizontal electrophoresis chamber and covered with 0.5cm of 1X Neutral Electrophoresis Buffer. Electrophoresis was carried out at the rate of 1.0 V/cm for 45 min. The slides were then removed and immersed in a DNA precipitation solution (1M NH4Ac, 95% EtOH) for 30min at room temperature before immersion in 70% EtOH for 30min at room temperature. The slides were air dried at 37C for 10-15min and stored at room temperature until ready for staining and imaging. Comet assay DNA slides were stained with 100ul of SYBR Gold dye (Thermo Fisher, 1:10,000 in Tris-EDTA buffer, pH 7.5) per area for 30 min at room temperature in the dark. Excess SYBR solution was removed by tapping and slides rinsed briefly in water before allowed to dry completely at 37C.

For each slide area, 50 randomly chosen comets were analyzed using a Nikon Ti-E with an excitation filter of BP 450–480 nm and a barrier filter of 515 nm. Fluorescent images of single cells were captured at 10X magnification and images were scored for comet parameters like the tail length and tail moment (% DNA in tail x tail length) using the OpenComet ImageJ plugin.

4.8. Class switch recombination assay

CSR was induced in CH12 cells as previously described (**CITATION**). CSR stimulation was done at 5x10^4 cells/ml in the presence of 20ng/ml IL-4 (Peprotech, 214-14), 1ug/ml anti-CD40 antibody (BD Biosciences, 553721), and 1 ng/ml rhTGF-beta 1 (R&D Systems, 240-B-010). Cells were harvested after 12, 24, or 48hr of stimulation for FACS analysis to detect class switching. Briefly, cells were resuspended and centrifuged at 1200 rpm for 5min at 4C, supernatant was removed, cells were resuspended in remaining ~100ul of medium by gentle vortexing. 100ul of FACS buffer (2.5% v/v FBS/PBS; filtered 0.2um) containing antibodies (Fisher Scientific, BD 559354) or no antibodies and incubated for 30min on ice in the dark. 1mL of FACS buffer was added to each tube before centrifugation at 1200 rpm for 5min at 4C, supernatant was poured off, cells were resuspended well in 300ul FACS buffer before analysis on a Moxi Flo (ORFLO MXF001). Analysis was performed with FlowJo.

Table 1. Nucleic acid sequences used in this study

20mer dsDNA 5FAM Anti-Sense	TATTGCTATAGAATTAACTT
20mer dsDNA 5FAM Sense	/56-FAM/AAGTTAATTCTATAGCAATA
20mer ssDNA 5FAM	/56-FAM/AAGTTAATTCTATAGCAATA
40mer dsDNA FAM Anti-Sense	TCGGCTAATCATGTTATCTAAATAAGTTGGGGTTTGCAGT
40mer dsDNA FAM Sense	/56-FAM/ACTGCAAACCCCAACTTATTTAGATAACATGATTAGCCGA
40mer ssDNA 5FAM	AGAAAGGAAGGTCCCCATACACCGACGCACCTGTTTACAC
60mer dsDNA 5FAM Anti-Sense	TGAAGGCTATATCCTATTGTTGACCTTGTGCATACATAATATGGTTTCGTACATGTAGCA
60mer dsDNA 5FAM Sense	/56-FAM/TGCTACATGTACGAAACCATATTATGTATGCACAAGGTCAACAATAGGATATAGCCTTCA
60mer ssDNA 5FAM	/56-FAM/TGCTACATGTACGAAACCATATTATGTATGCACAAGGTCAACAATAGGATATAGCCTTCA

5. REFERENCES

Andrin, C., McDonald, D., Attwood, K. M., Rodrigue, A., Ghosh, S., Mirzayans, R., Masson, J. Y., Dellaire, G., and Hendzel, M. J. (2012). A requirement for polymerized actin in DNA double-strand break repair. Nucleus 3(4), 384-95.

Aymard, F., Aguirrebengoa, M., Guillou, E., Javierre, B. M., Bugler, B., Arnould, C., Rocher, V., Iacovoni, J. S., Biernacka, A., Skrzypczak, M., Ginalski, K., Rowicka, M., Fraser, P., and Legube, G. (2017). Genome wide mapping of long range contacts unveils DNA double strand breaks clustering at damaged active genes. Nat Struct Mol Biol 24(4), 353-361.

Baarlink, C., and Grosse, R. (2014). Formin' actin in the nucleus. Nucleus 5(1), 15-20.

Baarlink, C., Plessner, M., Sherrard, A., Morita, K., Misu, S., Virant, D., Kleinschnitz, E.M., Harniman, R., Alibhai, D., Baumeister, S., Miyamoto, K., Endesfelder, U., Kaidi, A., and Grosse, R. (2017). A transient pool of nuclear F-actin at mitotic exit controls chromatin organization. Nat cell Bio 19(12), 1389-1399.

Belin, B. J., Cimini, B. A., Blackburn, E. H., and Mullins, R. D. (2013). Visualization of actin filaments and monomers in somatic cell nuclei. Mol Biol Cell 24(7), 982-94.

Belin, B. J., Goins, L. M., and Mullins, R. D. (2014). Comaprative analysis of tools for live cell imaging of actin network architecture. Bioarchitecture 4(6), 189-202.

Belin, B. J., Lee, T., and Mullins, R. D. (2015). DNA damage induces nuclear actin filament assembly by Formin-2 and Spire 1/2 that promotes efficient DNA repair. Elife 19, 07735.

Bohnsack, M. T., Stuven, T., Kuhn, C., Cordes, V. C., and Gorlich, D. (2006). A selective block of nuclear actin export stabilizes the giant nuclei of Xenopus oocytes. Nat Cell Biol 8(3), 257-63.

Caridi, C.P., D'Agostino, C., Ryu, T., Zapotoczny, G., Delabaere, L., Li, X., Khodaverdian, V. Y., Amaral, N., Lin, E., Rau, A. R., and Chiolo, I. (2018). Nuclear F-actin and myosins drive relocalization of heterochromatic breaks. Nature 559(7712), 54-60.

Dopie, J., Skarp, K. P., Rajakyla, E. K., Tanhuanpaa, K., and Vartiainen, M. K. (2012). Active

maintenance of nuclear actin by importin 9 supports transcription. Proc Natl Acad Sci USA 109(9), 544-52.

Du, J., Fan, Y. L., Chen, T. L., and Feng, X. Q. (2015). Lifeact and Utr230 induce distinct actin assemblies in cell nuclei. Cytoskeleton 72(11), 570-5.

Hatano, S., and Oosawa, F. (1966). Isolation and characterization of plasmodium actin. Biochim Biophys Act 127(2), 488-98.

Hinze, C., and Boucrot, E. (2018). Local actin polymerization during endocytic carrier formation. Biochem Soc Trans 46(3), 565-576.

Huet, G., Skarp, K. P., and Vartiainen, M. K. (2012). Nuclear actin levels as an important transcriptional switch. Transcription 3(5), 226-30.

Hurst, V., Shimada, K., and Gasser, S. M. (2019). Nuclear actin and actin-binding proteins in DNA repair. Trends Cell Biol 29(6), 462-476.

Iliakis, G., Mladenov, E., and Mladenova, V. (2019). Necessities in the processing of DNA double strand breaks and their effects on genomic instability and cancer. Cancers (Basel) 11(11), 1671.

Kapoor, P., Chen, M., Winkler, D. D., Luger, K., and Shen, X. (2013). Evidence for monomeric actin function in INO80 chromatin remodeling. Nat Struct Mol Biol 20(4), 426-32.

Kapoor, P., and Shen, X. (2013). Mechanisms of nuclear actin in chromatin-remodeling complexes. Trends Cell Biol 24(4), 238-46.

Lee, S. H., and Dominguez, R. (2010). Regulation of actin cytoskeleton dynamics in cells. Mol Cells 29, 311-325.

Lestourgeon, W. M., Forer, A., Yang, Y. Z., Bertram, J.S., and Pusch, H. P. (1975). Contractile proteins. Major components of nuclear and chromosome non-histone proteins. Biochim Biophys Acta 379(2), 529-52.

Liu, T., and Huang, J. (2016). DNA end resection: facts and mechanisms. Genomics Proteomics Bioinformatics 14(3), 126-130.

Matsuoka, S., Ballif., B. A., Smogorzewska, A., McDonald III, E. R., Hurov, K. E., Luo, J., Bakalarski, C. E., Zhao, Z., Solimini, N., Lerenthal, Y., Shiloh, Y., Gygi, S. P., and Elledge, S. J. (2007). ATM and ATR substrate analysis reveals extensive protein networks responsive to DNA damage. Science 316(5828), 1160-6.

Montaville, P., Kuhn, S., Compper, C., and Carlier, M. F. (2016). Role of the C-terminal extension of Formin 2 in its activation by spire protein and processive assembly of actin filaments. J Biol Chem 291(7), 3302-18.

Olave, I. A., Reck-Peterson, S. L., and Crabtree, G. R. (2001). Nuclear actin and actin-related proteins in chromatin remodeling. Annu Rev Biochem 71, 755-81.

Pederson, T., and Aebi, U. (2002). Actin in the nucleus: what form and what for? J Struct Biol 140(1-3), 3-9.

Philimonenko, V. V., Zhao, J., Iben, S., Dingova, H., Kysela, K., Kahle, M., Zentgraf, H., Hofmann, W. A., de Lanerolle, P., Hozak, P., and Grummt, I. (2004). Nuclear actin and myosin I are required for RNA polymerase I transcription. Nat Cell Biol 6(12), 1154-72.

Plessner, M., Melak, M., Chinchilla, P., Baarlink, C., and Grosse, R. (2015). Nuclear F-actin formation and reorganization upon cell spreading. J Biol Chem 290(18), 11209-16.

Plessner, M., and Grosse, R. (2015). Extracellular signaling cues for nuclear actin polymerization. Eur J Cell Biol 94(7-9), 359-62.

Pollard, T. D., Blanchoin, L., and Mullins, R. D. (2000). Molecular mechanisms controlling actin filament dynamics in nonmuscle cells. Annu Rev Biophys Biomol Struct 29, 545-76.

Pollard, T. D., and Borisy, G. G. (2003). Cellular motility driven by assembly and disassembly of actin filaments. Cell 112, 453-465.

Quinlan, M. E., Hilgert, S., Bedrossian, A., Mullins, R. D., and Kerkhoff, E. (2007). Regulatory interactions between two actin nucleators, Spire and Cappuccino. J Cell Biol 179(1), 117-28.

Schrank, B. R., Aparicio, T., Li, Y., Chang, W., Chait, B. T., Gundersen, G. G., Gottesman, M.

E., and Gautier, J. (2018). Nuclear Arp2/3 drives DNA break clustering for homology-directed repair. Nature 559(7712), 61-66.

Shibata, A. (2017). Regulation of repair pathway choice at two-ended DNA double-strand breaks. Mutat Res 803-805, 51-55.

Straub, F.B., and Szent-Gyorgyi, A. (1942). in Studies from the Institute of Medical Chemistry University Szeged Vol. 2, 3-15.

Steinbacher, T., and Ebnet, K. (2018). The regulation of junctional actin dynamics by cell adhesion receptors. Histochem Cell Biol 150(4), 341-350.

Thiam, H. R., Vargas, P., Carpi, N., Crespo, C. L., Raab, M., Terriac, E., King, M. C., Jacobelli, J., Alberts, A. S., Stradal, T., Lennon-Dumenil, A. M., and Piel, M. (2016). Perinuclear Arp2/3-driven actin polymerization enables nuclear deformation to facilitate cell migration through complex environments. Nature Communications 7; 10997.

Treisman, R. (2013). Shedding light on nuclear actin dynamics and function. Trends Biochem Sci 38, 376-377.

Vartiainen, M. K., Guettler, S., Larijani, B., and Treisman, R. (2007). Nuclear actin regulates dynamic subcellular localization and activity of the SRF cofactor MAL. Science 316(5832), 1749-52.

Vitor, A. C., Huertas, P., Legube, G., and Almeida S. F. (2020). Studying DNA double-strand break repair: an ever-growing toolbox. Front Mol Biosci 2, 7-24.

Yamada, K., Ono, M., Perkins, N. D., Rocha, S., and Lamond, A. I. (2013). Identification and functional characterization of FMN2, a regulator of the cyclin-dependent kinase inhibitor p21. Mol Cell 49-(5), 922-33.

Yoo, Y., Wu, X., and Guan, J.L. (2007). A novel role of the actin-nucleating Arp2/3 complex in the regulation of RNA polymerase II-dependent transcription. J Biol Chem 282(10), 7616-23.

Zuchero, J. B., Belin, B., and Mullins, R. D. (2012). Actin binding to WH2 domains regulates

nuclear import of the multifunctional actin regulator JMY. Mol Biol Cell 23(5), 853-63.

Publishing Agreement

It is the policy of the University to encourage open access and broad distribution of all theses, dissertations, and manuscripts. The Graduate Division will facilitate the distribution of UCSF theses, dissertations, and manuscripts to the UCSF Library for open access and distribution. UCSF will make such theses, dissertations, and manuscripts accessible to the public and will take reasonable steps to preserve these works in perpetuity.

I hereby grant the non-exclusive, perpetual right to The Regents of the University of California to reproduce, publicly display, distribute, preserve, and publish copies of my thesis, dissertation, or manuscript in any form or media, now existing or later derived, including access online for teaching, research, and public service purposes.

DocuSigned by:
Terri Lee
57CAEB67C1FC406...
Author Signature

9/3/2020
Date